Table I. NMR Spectroscopic Data (δ) for Selected Complexes[a,b]

complex	H_α	H_β	C_5H_5	$C(CH_3)_3$	$^{13}C_\alpha$	^{31}P
2a	9.07 (1 H, t, J = 7.0 Hz)	1.88 (2 H, d, J = 7.0 Hz)	6.06 (5 H, s) 6.02 (5 H, s)	0.53 (9 H, s)		
2b	8.63 (1 H, t, J = 6.7 Hz)	2.34 (2 H, d, J = 6.7 Hz)	6.09 (10 H, s)	0.46 (9 H, s)		
3a	11.71 (1 H, ddd, J = 12.0, 5.5, 4.1 Hz)	3.66 (1 H, ddd, J = 12.0, 15.7, 2.3 Hz) 2.87 (1 H, ddd, J = 15.7, 5.5, 7.4 Hz)	5.49 (5 H, d, J = 1.4 Hz) 5.42 (5 H, d, J = 1.4 Hz)	1.03 (9 H, s)	270	55.2
3a''	9.88 (1 H, t, J = 8.9 Hz)	3.47 (2 H, d, J = 8.9 Hz)	5.87 (10 H, s)	1.02 (9 H, s)	230	29.4
5	12.04 (2 H, d, J = 6.0 Hz)		5.34 (10 H, d, J = 2.2 Hz)		287	38.1

[a] ^{1}H NMR chemical shift data for the coordinated phosphine or HMPA have been omitted. [b] See ref 8.

Table II. Product Yields in Alkylidene Transfer Reactions[a]

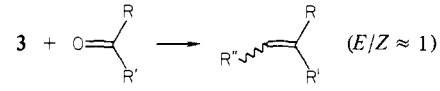

complex	carbonyl compd	product	yield, %
3a	cyclohexanone	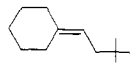	≈quantitative
3a	γ-butyrolactone	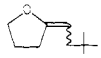	≈quantitative
3a'			70
3a''			97
3a	methyl benzoate	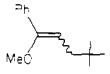	94
3b	γ-butyrolactone	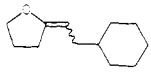	84
3c	γ-butyrolactone	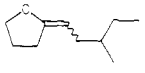	78
3e	γ-butyrolactone	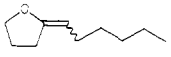	80

[a] Yields were determined by GLC and are based on 3.

Table III

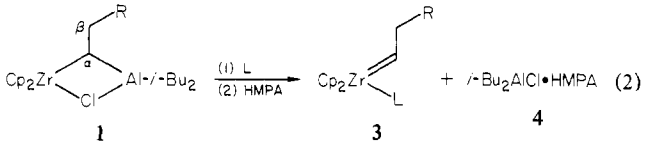

1 3 4

complex	R	complex	L	yield, %[a]
1a		3a	PPh_3	54
		3a'	PMe_2Ph	70
		3a''	HMPA[b]	69
1b		3b	PPh_3	39
		3b'	PMe_2Ph	59
1c		3c	PPh_3	33
		3c'	PMe_2Ph	52
1d	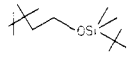	3d	PMe_2Ph	30
1e	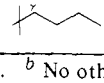	3e	PPh_3	8
		3e'	PMe_2Ph	10

[a] See ref 14. [b] No other phosphine ligand added.

groups at the γ position may hamper attainment of a favorable configuration for hydride elimination to aluminum and thus may allow carbene complex formation to compete with it.[17,18]

Zirconium and titanium carbene complexes formed with alkylidene precursors are active "Wittig-type" reagents. Both convert esters to vinyl ethers and ketones to olefins in 78–100% yield.[19] For the Zr compounds the reaction is carried out at 70 °C for 6 h. The more reactive Ti species requires only 2–3 h at room temperature for complete reaction to occur.

Acknowledgment. We acknowledge support for this work by the National Science Foundation and the National Institutes of Health.

(16) McDermott, J. X.; White, J. F.; Whitesides, G. M. *J. Am. Chem. Soc.* **1973**, *95*, 4451.

(17) In fact, ^{1}H NMR analysis of methine α and β proton splitting patterns for **1a–c**, and **1e** reveals an interesting correlation between the structure of the bridging alkylidene species and the yield of the carbene complex derived from it. For **1a**, H_α is observed as a doublet of doublets ($^3J_{H_\alpha H_\beta}$ = 4.0 Hz, $^3J_{H_\alpha H_{\beta'}}$ = 11.4 Hz), which suggests hindered rotation about the C_α–C_β bond of the alkyl chain. As the size of the alkyl group γ substituent decreases, this splitting pattern evolves toward and then becomes an apparent triplet (for **1b**, $^3J_{H_\alpha H_\beta}$ = 4.0 Hz, $^3J_{H_\alpha H_{\beta'}}$ = 12.0 Hz; for **1e**, $^3J_{H_\alpha H_\beta}$ = 7.3 Hz, $^3J_{H_\alpha H_{\beta'}}$ = 9.2 Hz; for the ethylidene-bridged analogue, a triplet is observed, $^3J_{H_\alpha H_{\beta'}}$ = 8 Hz), consistent with the notion of increasing facility of C_α–C_β bond rotation.

(18) An alternative explanation of the size–yield relationship is that dimerization of the coordinatively unsaturated carbene complex formed by reaction of **1** with HMPA becomes favorable relative to ligand trapping as the steric bulk of the alkyl chain decreases. The observation that the yield of carbene complex does not vary with a 2-fold increase in phosphine ligand trap concentration argues against this hypothesis.

(19) In a typical reaction 1 mmol of a 0.2 M toluene solution of **3a** was added to 1 equiv of a 0.5 M toluene solution of butyrolactone at 50 °C over 10 min. Heating was maintained at 70 °C for 6 h. Workup according to a reported procedure (Pine, S. H.; Zahler, R.; Evans, D. A.; Grubbs, R. H *J. Am. Chem. Soc.* **1980**, *102*, 3270) gave an ethereal solution from which yields were obtained by GLC analysis. Organic products were also isolated and identified by GC–MS and ^{1}H NMR spectroscopy.

Solid-State Rearrangement of (Phenylazophenyl)palladium Hexafluoroacetylacetonate

M. C. Etter* and A. R. Siedle*

Science Research Laboratory
3M Company, St. Paul, Minnesota 55101

Received September 20, 1982

Polymorphic transformations and solid-state chemical reactions, some of them of surprising complexity, are well documented for organic materials,[1] and the scope and importance of organic solid-state chemistry is now well established.[2] Organometallic solid-state reactions have, on the other hand, only rarely been studied.[3] We report a novel rearrangement of (phenylazo-

(1) (a) Scheffer, J. R. *Acc. Chem. Res.* **1980**, *13*, 283. (b) Paul, I. C.; Curtin, D. Y. *Ibid.* **1973**, *6*, 217.

(2) (a) Gavezzoti, A.; Simonetta, M. *Chem. Rev.* **1982**, *82*, 1. (b) Cohen, M. D.; Green, B. S. *Chem. Br.* **1973**, *9*, 490.

0002-7863/83/1505-0641$01.50/0 © 1983 American Chemical Society

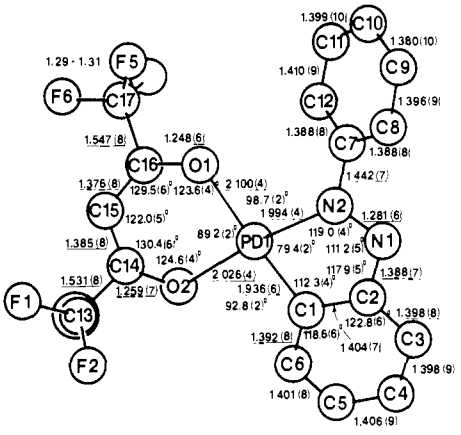

Figure 3. Bond lengths and angles for one of the two independent molecules in the unit cell of **1**.

phenyl)palladium hexafluoroacetylacetonate that demonstrates that solid-state organometallic chemistry is a promising area for future research.

This compound is obtained by cyclometalation of azobenzene with palladium bis(hexafluoroacetylacetonate).[4] Cooling a hexane solution, saturated at room temperature, provides faintly dichroic acicular yellow crystals of **1**, λ_{max} 415 nm. Thermal transformations of these crystals were followed by using differential scanning calorimetry and a hot-stage microscope fitted with a video tape recorder. When crystals of **1** are heated to 90 ± 10 °C,[5] they undergo a sudden discontinuous expansion of about 10% along the needle axis with no measureable change in width. If the crystals are heated on only one face, sufficient mechanical strain develops that they literally fly off the hot stage. Weissenberg X-ray photographs of the expanded crystals at this point show only the diffraction pattern of **1**, but the reflections are now highly extended (up to 20° in ω), indicating a disordered lattice. On further heating, a red phase front develops at one end of the crystal and moves along the needle axis until the entire crystal is an opaque red color, λ_{max} 480 nm. Then at 157 °C, the red crystals melt. ΔH for both the expansion and the color change, determined by differential scanning calorimetry, is 2.1 kcal/mol (see Figure 1, supplementary material); no weight change is detected by thermal gravimetric analysis. The elemental analyses and infrared spectra of the red polymorph **2** so produced match those of **1**, but X-ray powder patterns and the optical spectra (Figure 2, supplementary material) are different. Although the solid-state rearrangements are irreversible, the two polymorphs can be interconverted by recrystallization from solvents such as hexane, chloroform, or xylene.

Weissenberg patterns indicated that **2** obtained by solid-state transformation of single crystals of **1** exists as a microcrystalline phase. Single crystals of the red polymorph can be obtained by recrystallization of **1** from hot xylene, and their X-ray powder patterns match those of **2** obtained by thermally transforming **1** in the solid state.

X-ray single-crystal diffraction studies of **1** and **2**[6] show that

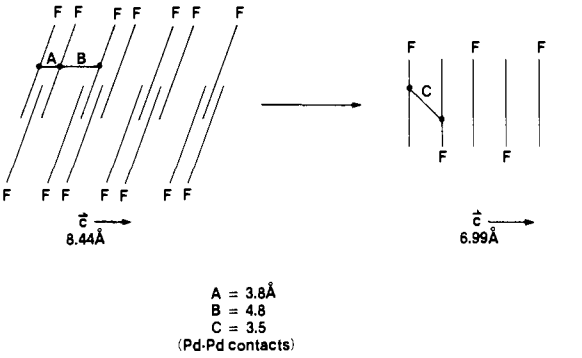

Figure 4. Schematic diagram of the packing pattern of the polymorphic forms **1** and **2**, showing the Pd–Pd contact distances and directions and the orientations of molecular stacks. The molecules are represented by straight lines indicating the mean plane of the molecule and F representing the end of the molecule with the F_6acac groups. The structure of **1** is shown on the left, with the observed crystal expansion direction parallel to the *c* axis of **1**, as indicated.

Chart I

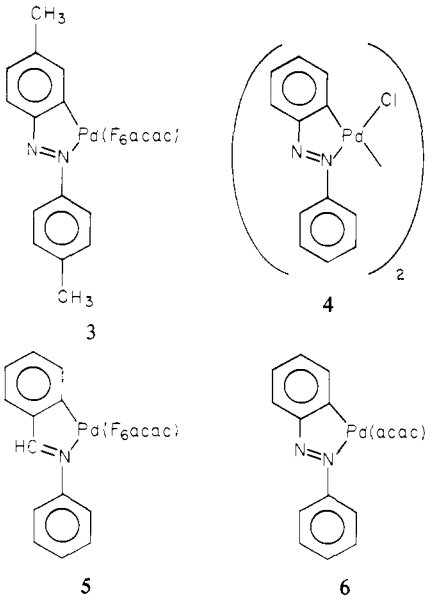

these forms both are triclinic and are indeed polymorphs, with **1** containing two crystallographically independent molecules while **2** has only one molecule per asymmetric unit. The torsion angles about the N2–C7 bond to the exocyclic phenyl ring are 46.5 and 46.2° for **1** and 14.5° for **2**. The N=N distances in the two molecules of **1** are 1.262 (6) and 1.281 (6) Å, slightly longer than N=N in *trans*-azobenzene, 1.236 (6) Å.[7] In **2**, the N=N distance is 1.277 Å. The Pd–C separations are 1.936 (6) and 1.938 (6) Å for **1** and 1.997 Å for **2**. The Pd–O distances within each molecule are not equal as previously observed in similar complexes.[8] In Figure 3, the intramolecular geometry for one of the molecules in structure **1** is shown. In **2**, the thermal ellipsoids associated with the fluorine atoms are much larger than for the fluorines in **1**, correlating with a lower calculated density for **2** (1.84 vs. 1.90 g/cm^3).

Despite the similarities in molecular structure between **1** and **2** and the fact that they are both in the same space group, their packing patterns are markedly different. **1** packs such that alternating Pd–Pd contacts of 3.8 and 4.8 Å occur along the *c* axis direction (which is also the needle axis of the crystal). In Figure

(3) (a) Green, M.; Howard, J. A. K.; Mills, R. M.; Pain, G. N.; Stone, F. G. A. *J. Chem. Soc., Chem. Commun.* **1981**, 869. (b) Raston, C. L.; White, A. H. *J. Chem. Soc., Dalton Trans.* **1976**, 7. (c) Lyerla, J. R.; Fyfe, C. A.; Yannoni, C. S. *J. Am. Chem. Soc.* **1979**, *101*, 1351. (d) Bielli, E.; Gidney, P. M.; Gillard, R. D.; Heaton, B. T. *J. Chem. Soc., Dalton Trans.* **1974**, 2133.

(4) Siedle, A. R. *J. Organomet. Chem.* **1981**, *208*, 115.

(5) The precise temperature of the phase transition depends on the degree of crystal perfection and mechanical history, e.g., particle size and extent of grinding.

(6) Crystal data. **1**: $P\bar{1}$, a = 13.205 (3) Å, b = 15.715 (3) Å, c = 8.436 (3) Å, α = 93.61 (2)°, β = 86.98 (2)°, γ = 95.40 (2)°, Z = 4, V = 1737 Å^3, R = 0.045, and R_w = 0.048, using 3891 reflections (506 variables) for which $F_o^2 \geq 3\sigma(F_o)^2$. **2**: $P\bar{1}$, a = 11.677 (2) Å, b = 12.465 (2) Å, c = 6.992 (3) Å, α = 95.20 (2)°, β = 63.11 (1)°, γ = 98.80 (2)°, Z = 2, V = 897 Å^3, R = 0.094, and R_w = 0.096, using 1543 reflections (251 variables) for which $F_o^2 \geq 3\sigma(F_o)^2$. For both crystals, Mo Kα radiation (λ = 0.71069 Å) and 0 < 2θ < 50° scans were employed. Programs used in the structure solutions were from the "Enraf-Nonius Structure Determination Package"; Molecular Structure Corp.: College Station, TX, 3rd ed.; 1978.

(7) Brown, C. J. *Acta, Crystallogr.* **1966**, *21*, 146.

(8) Siedle, A. R.; Pignolet, L. H. *Inorg. Chem.* **1981**, *20*, 1849.

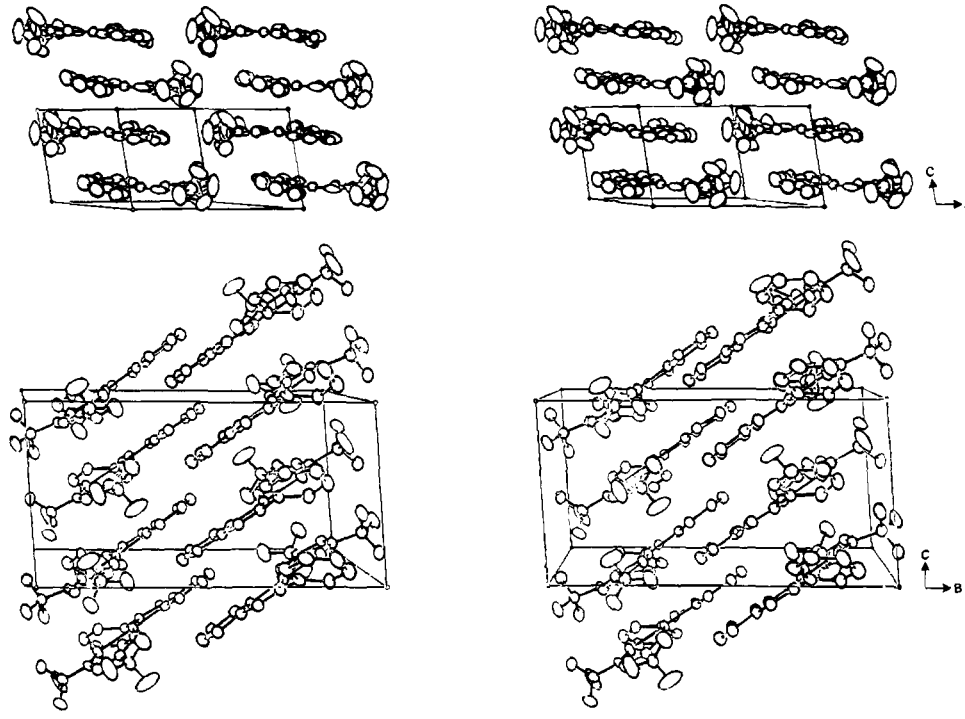

Figure 5. Stereopair views of the crystal packing patterns of triclinic **1** and **2**, viewed along [100] for **1** (top) and along [010] for **2**. **1** has two molecules per asymmetric unit, while **2** has only one.

4, a schematic pattern of the molecular packing shows how the *i*-related molecular stacks are interleaved in the structure of **1**. The red polymorph contains *i*-related molecules within a stack. In this structure, the Pd-Pd distance between neighboring molecules is 3.5 Å, and the molecular stack is parallel to the *c* axis (also the long axis of the red crystal plates). These packing pattern differences are seen in the stereopair views of the two structures in Figure 5.

On the basis of these structures and their relationship to the observed crystal expansion, we propose that the neighboring *i*-related molecular stacks in **1** slip together, as in a Martensitic transformation,[9] by moving along [011] in the direction of the long axis of the molecules. This would cause crystal fracture along the [010] planes, which is observed when thin crystals are heated. The crystal expansion occurs along the *c* axis (the needle axis) as expected from this mechanism. It remains a puzzle that the red color of **2** develops subsequent to rather than simultaneously with the expansion process. There are no unusually short intermolecular contacts in **2** that could account for the color change. This longer wavelength absorption may be due to the more extended conjugation in the planar conformation of **2**.[10] Since differential scanning calorimetry of the closely related molecules **3-6** (Chart I) reveals no solid-state rearrangements, it is clear that the solid-state changes observed for **1** are not due to any obvious property of the molecule itself but result from subtle packing properties which are not readily characterized. Anomalies such as these indicate that major advances in the field of solid-state chemistry are still needed in order to correlate molecular structure, crystal packing modes, and solid-state chemical and physical properties.

Acknowledgment. We thank Profs. R. D. Gillard and G. Wegner for their helpful discussions and suggestions and the staff of the 3M Analytical and Properties Research Laboratory (D. Markoe, W. Bahmet, G. Lillquist) for the DSC, powder diffraction, and Raman data.

Registry No. 1, 84074-20-4; azobenzene, 103-33-3; palladium bis(hexafluoroacetylacetonate), 65353-51-7.

Supplementary Material Available: Tables of atomic coordinates and temperature factors and Figures 1 and 2 (5 pages). Ordering information is given on any current masthead page.

(9) (a) Smoluchowski, R., Mayer, J. E., Weyl, W. A., Eds. "Phase Transformations in Solids"; Wiley: New York, 1951: Chapter 1. (b) Private conversation with Prof. G. Wegner, who suggested the analogy between this transformation and a Martensitic transformation.

(10) Preliminary Raman data indicate that the 1375-cm^{-1} N=N stretching band in solid **2** is resonance enhanced and, therefore, coupled to the long-wavelength transition. Following the arguments of Vrieze and coworkers, this suggests that the 480-nm absorption is, as proposed, connected with the diazo group.[11,12]

(11) VanBaar, J. F., Vrieze, K.; Stufkens, D. J. *J. Organomet. Chem.* **1975**, *85*, 249.

(12) VanBaar, J. F.; Vrieze, K.; Stufkens, D. J. *J. Organomet. Chem.* **1975**, *97*, 461.

Design of Organic Metals Based on Tetramethyltetraselenafulvalene: Novel Structural Implications and Predictions

Jack M. Williams,* Mark A. Beno, James C. Sullivan, Lisa M. Banovetz,† Julie M. Braam,† Gregory S. Blackman,† Clark D. Carlson,† Deena L. Greer,† and Diana M. Loesing†

Chemistry Division, Argonne National Laboratory Argonne, Illinois 60439

Received August 23, 1982

Presently at least six $(TMTSF)_2X$ metals, X = TaF_6^-, SbF_6^-, AsF_6^-, PF_6^-, ReO_4^-, and ClO_4^- where TMTSF = tetramethyltetraselenafulvalene, are reported superconductors.[1] All derivatives have superconducting (SC) T_c's $\simeq$ 1 K, and except for $(TMTSF)_2ClO_4$, the only *ambient-pressure*[2] organic superconductor known, they all require an applied pressure of ~8-12 kbar in order to induce the SC state. Although all reported

† Research participation student under the auspices of the Division of Educational Programs, Argonne National Laboratory.

(1) For a general discussion of TMTSF metals see: *Mol. Cryst. Liq. Cryst.* **1982**, *79*, 1-359. TMTSF is $\Delta^{2,2'}$bi-4,5-dimethyl-1,3-diselenolylidene.

(2) Bechgaard, K.; Carneiro, K.; Rasmussen, F. B.; Olsen, M.; Rindorf, G.; Jacobsen, C. S.; Pedersen, H. J.; Scott, J. C. *J. Am. Chem. Soc.* **1981**, *103*, 2440.

0002-7863/83/1505-0643$01.50/0 © 1983 American Chemical Society